

Background

> Spontaneous otoacoustic emissions (SOAEs) provide a useful (but indirect) means to probe the "active" ear

> Theoretical models based on limit cycle oscillators (Fig.1) have provided valuable insight into underlying nonlinear features [e.g., Johannesma, 1980; Wit, 1985; Talmadge et al. 1991; Hudspeth, 2008]

> Recent efforts have considered collections of coupled limit cycle oscillators [e.g., Duke & Julicher, 2003; Fruth et al. 2014], but much remains poorly understood given the wide variety of parameters and coupling configurations

> One model class [Vilfan & Duke, 2008; Gelfand et al. 2010], inspired by the lizard ear and extended to humans [Wit & van Dijk, 2012], considers nearest-neighbor coupling (Fig.2) and the notion of "clusters" (groupings of self-entrained oscillators)

> This model type however fails to qualitatively produce features of SOAE activity [Salerno & Bergevin, 2015; see Fig.6], perhaps in part due to unrealistic biomechanical coupling assumptions

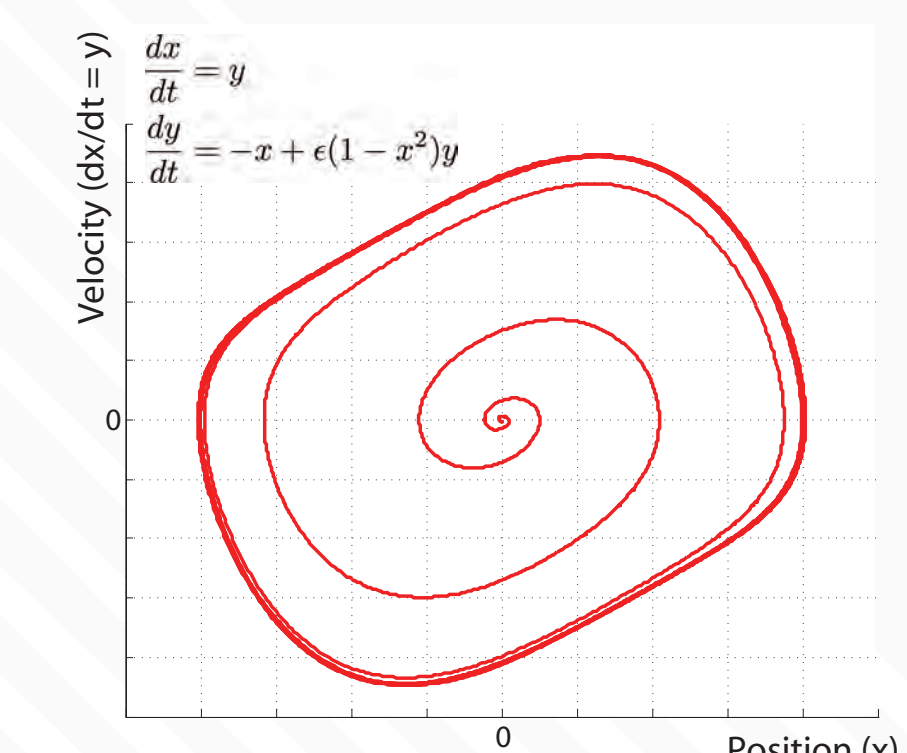


FIGURE 1 - Phase plane picture of a limit cycle for the "self sustained" van der Pol oscillator

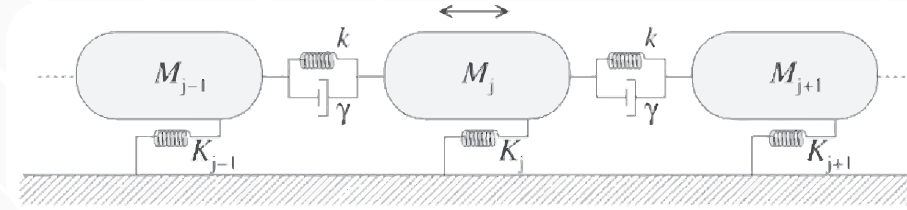


FIGURE 2 - Basic schematic for nearest-neighbor coupled model [Vilfan & Duke, 2008]

Goal

Focusing on the relatively simpler ear of a lizard (Fig.3), we develop a theoretical foundation that **combines active nonlinear oscillators** [Vilfan & Duke, 2008] **with global coupling via the rigid papilla** [Bergevin & Shera, 2010]. This model (Fig.4, Eqns.1) is then used to **help interpret data characterizing the dynamics of SOAE activity** (e.g., response to swept tones, tone bursts) and the connection to stimulus frequency emissions (SFOAEs). A characteristic empirical focal point is the **"ring of fire"** (Fig.5).

OAE Methods

• All measurements were made using an Etymotic ER-10C probe system, connected to a PC running custom software. All data was sampled at 44.1 kHz at 24 bits. Lizards were lightly anesthetized and kept at a stable body temperature via a heating blanket. Earphones were calibrated in-situ. Tone-bursts were cosine-ramped to minimize spectral splatter.

• Analysis was performed using custom software written in Matlab. Two primary methods employed were the Fourier and Hilbert transforms. Spectrogram analyses were done via a short-time Fourier transform, whose parameters (window type, segment length, fractional overlap) were chosen with the goal of optimizing time-frequency resolution.



FIGURE 3 - Lizard (*Anolis carolinensis*) used for this study. Some morphological properties of the inner ear:
> BM Length: ~0.5 mm
> Hair cell count: ~160
> TM: None (over most of papilla)
> BM traveling wave: No

Model

• Numerical simulations were run in Matlab using the equations specified below (Eqns.1), solved using ode45 (4th order Runge-Kutta w/ adaptive step-size)

• Static irregularity ("roughness") was built into several model parameters: variations in coupling strengths (d_{ij} , d_j), active strength (ϵ_j), deviations from exponential tonotopic map (ω_j), and strength of nonlinearity (B_j)

• Model parameters (unless noted otherwise) are as follows: $N=100$ oscillators; tonotopic map is exponential w/ frequencies $\omega_j=1-4.5$ "Hz" and 2% noise; $d_{ij}=0.15$ and $d_j=1$, both w/ 5% noise; $B_j=1$; $\epsilon_j=1$ w/ 5% noise; $\kappa_j=1$; $\omega_j=2$ "Hz"; $\epsilon_j=-1$; $d_{ij}=0.15$ and $d_j=1$; $\alpha=\beta=1$. Unless noted, $L_i=L_j=0$.

• Initial conditions were random and sufficient time was allowed for settling. "SOAE" spectra could be obtained either from the papilla response or summing all active oscillators.

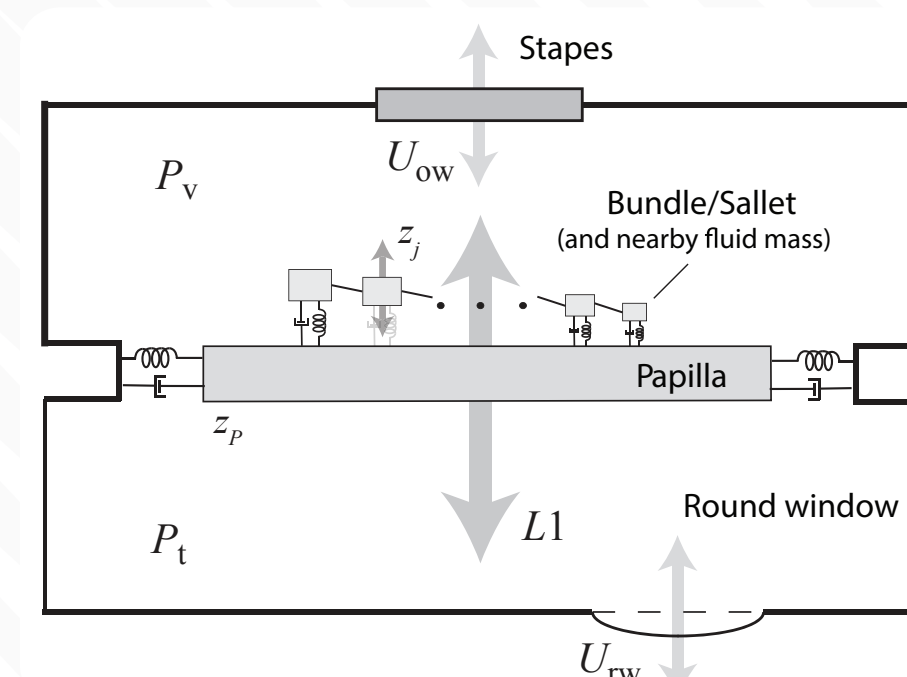


FIGURE 4 - Model schematic for lizard ear (cf. Bergevin & Shera, 2010; Vilfan & Duke, 2008). Here, individual "bundles" can be coupled in two different ways: either locally via nearest-neighbor connections (e.g., fluid boundary layer, elastic tectorium) or globally via the (relatively rigid) papilla.

$$\dot{z}_p = z_p(i\omega_p + \epsilon_p) + \alpha \sum_j^N d_{RP_j} (z_p - z_j) + i\beta \sum_j^N d_{IP_j} (z_p - z_j) + L_P(t)$$

$$\dot{z}_j = z_j(i\omega_j + \epsilon_j - B_j|z_j|^2) + \kappa_j(d_{R_j} + id_{I_j})(z_{j+1} + z_{j-1} - 2z_j) \dots + \alpha d_{RP} (z_j - z_p) + i\beta d_{IP} (z_j - z_p) + L_j(t)$$

Eqns.1 - Combination of Vilfan & Duke (2008) and Bergevin & Shera (2010). Rigid papilla (denoted P) acts as a passive harmonic oscillator, globally coupling the "bundles" (limit cycle oscillators, denoted j). Note that z is complex. All parameters are constant, except for non-autonomous terms L . Coupling to the middle ear is ignored. Equations slightly different for oscillators on the ends.

Eqns.2 - For reference, complex-valued 1st order ODE used here is equivalent to real-valued 2nd order ODE (with appropriate change of variables).

$$\dot{z} = -\gamma'z + i\omega'z + F(t)$$

$$\ddot{x} = -\gamma\dot{x} - \omega^2x + F(t)$$

Results

Hearing..... "is a burning thing, and it makes, a fiery ring". [Johnny Cash]

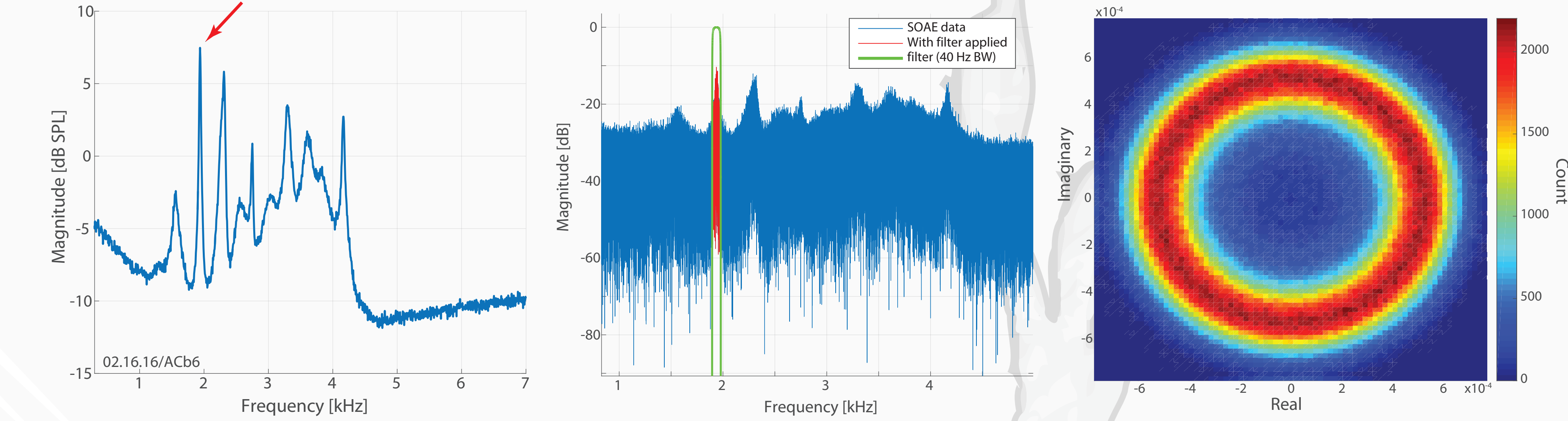


FIGURE 5 (Lizard) - The ring of fire. [Left] SOAE spectra from an anole, computed by averaging the magnitudes of four hundred 0.19 s sequential buffers (~74 s total). [Middle] Spectra of entire waveform, indicating filtering of one specific peak (red; filter properties indicated in green). [Right] Distribution of the filtered analytic signal of the filtered peak [Shera, 2003; Bergevin et al. 2015]

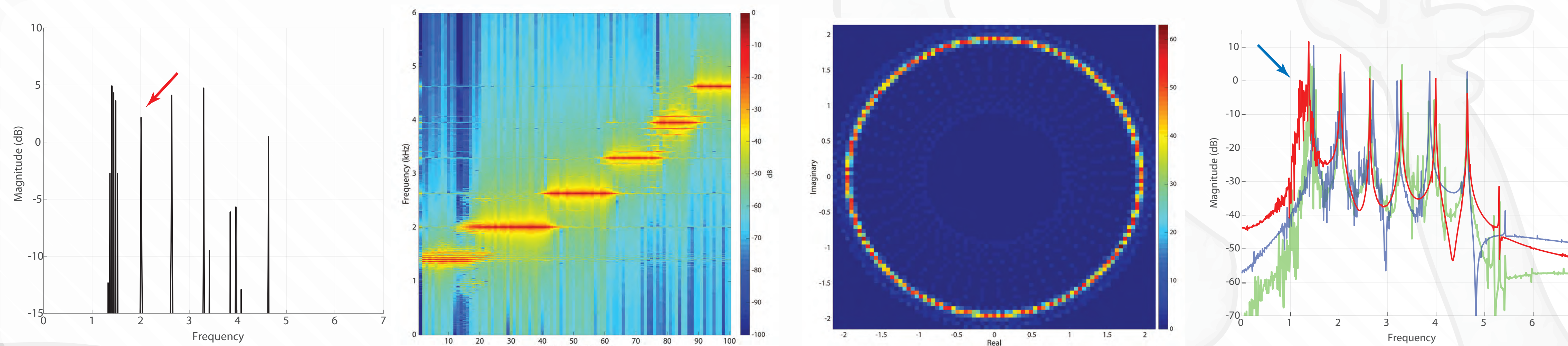


FIGURE 6 (Model) - Model spectra. [Left] Representative "SOAE" spectra, using similar scale as Fig.5. [Mid Left] Spectra for all the oscillators comprising the left figure. [Mid Right] "Ring of fire" for one peak (red arrow). [Right] Spectra for several different "roughness" patterns. Green trace is the same as left panel. Note zoomed-out scale.

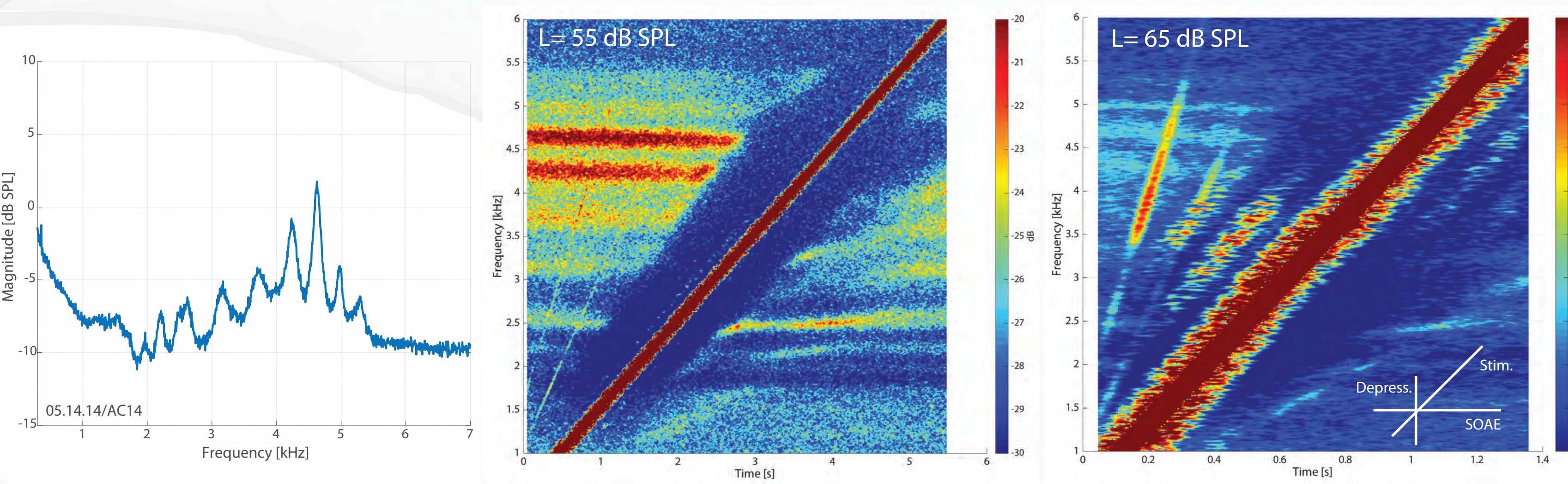


FIGURE 7 (Lizard) - Breaking the ring of fire w/ swept tones. Spectrograms of tones swept across frequency at constant peak level (55 dB SPL middle, 65 dB on right). Note that here the "ring(s) are unrolled and appear as horizontal lines. Sweep rate was 1 kHz/s. Spectrograms used a 4096 point window with 95% sliding overlap, spectrally averaged across 35 stimulus presentations. Left panel shows SOAE spectrum for this ear.

Summary of Results

- Consideration of SOAEs peaks through the lens of the "ring of fire" (Fig.5) provides a useful conceptual foundation. Additional "ring" dynamics are of interest (e.g., envelope fluctuations), but not considered here
- Model (Fig.6) is able to qualitatively capture some SOAE features, but not others (e.g., peak width, "baseline"). "Roughness" is not required per se for generation of "clusters", but may help produce more realistic peak widths
- Swept tones (Fig.7) cause broad regions of "depression" (i.e., decreased SOAE activity). Also, (sub-)harmonics stimulate matched SOAE activity.
- Tone bursts swept across frequency (Fig.8) indicate frequency pulling/pushing, and eventually "breaking" of SOAE peaks
- Tone bursts swept across level (Fig.9) show qualitatively similar behavior, including facilitation
- Model simulation w/ an external tone (Fig.11) indicates entrainment of closely tuned oscillators & breakup of clusters far away
- Growth of SFOAEs is relatively nonlinear (Fig.10), especially close to large SOAE peaks

Discussion

> Model does not (yet) readily account for qualitative properties, such as the the width apparent in the "ring of fire" or "baseline" emissions [Manley et al. 1996], even with global coupling

> Model suggests a possible mechanism by which SOAE spectra are depressed by external tones (Figs.7-9). In addition to entraining or suppressing activity, external tones can also cause a loss of phase coherence [Bergevin et al. 2015] amongst clustered groups (Fig.11). Thereby, **"depressed" regions are due to a mix of entrainment, suppression, & decoherence.**

> Tri-fold interpretation of SOAE depression could be consistent w/ nonlinear SFOAE growth (Fig.11), though further study is needed [e.g., Wit et al. 2012].

> Apparent from Figs.8&9, the timecourse of SOAE depression (and subsequent "release") is relatively fast (ms or shorter). Also, **SOAE spectra are highly stable overall**, even after strong forcing

> Model suggests (Fig.6, red curve) that static irregularity in strength of active term could allow for more realistic peak widths: i.e., not all hair cells are created equal, some being stronger than others and thereby acting like **"bullies in a gang"**. Put another way, every SOAE "peak" compositionally unique.

> Stimulus paradigm used here (Figs.8-9) can provide a relatively rapid estimate of **"SOAE STCs"** (suppression tuning curves), though **mix of contributing depression effects and idiosyncratic peak composition makes interpretation of such difficult**

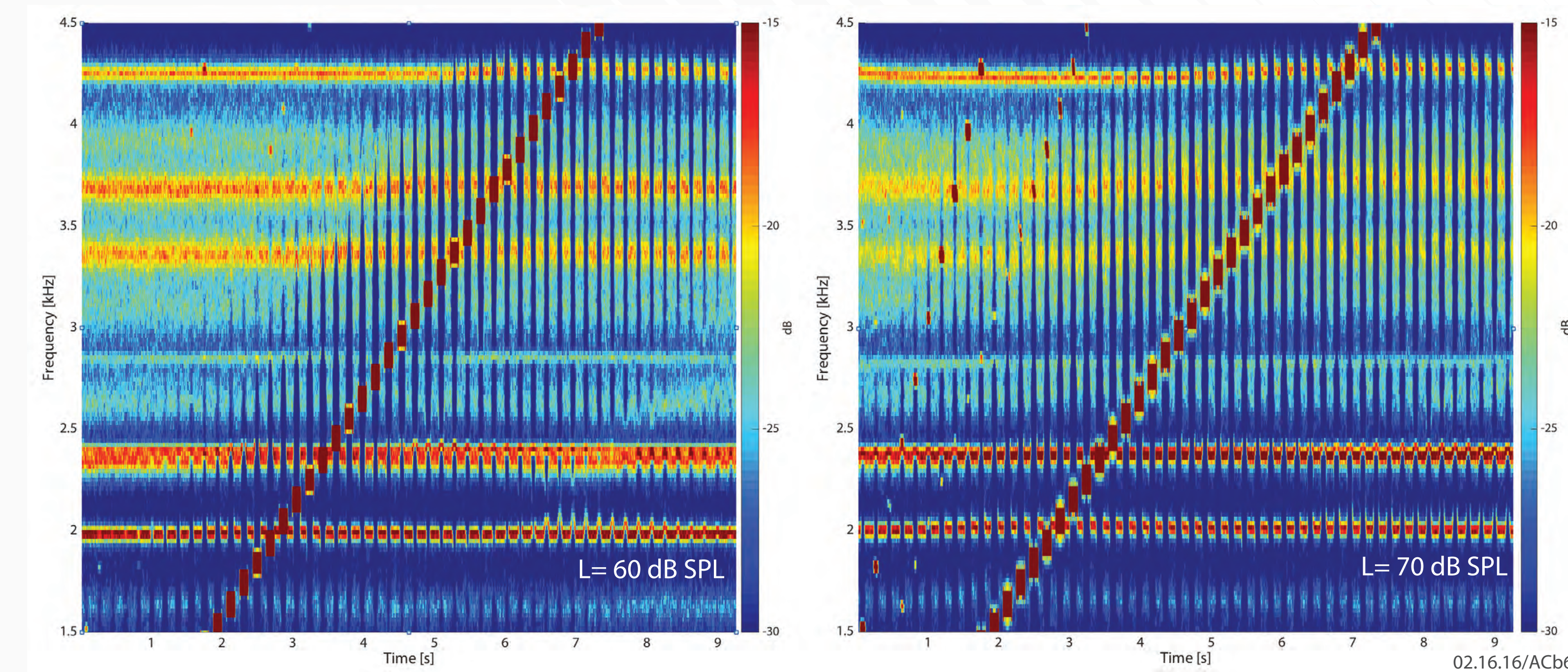


FIGURE 8 (Lizard) - Breaking the ring of fire w/ swept tone bursts. Spectrograms of tone burst swept across frequency at constant peak level (60 dB SPL on left, 70 dB on right). Bursts were 113 ms long, cosine-ramped. Spectrograms used a 2048 point window with 95% sliding overlap, spectrally averaged across 40 stimulus presentations. (same ear as shown in Fig.5,9)

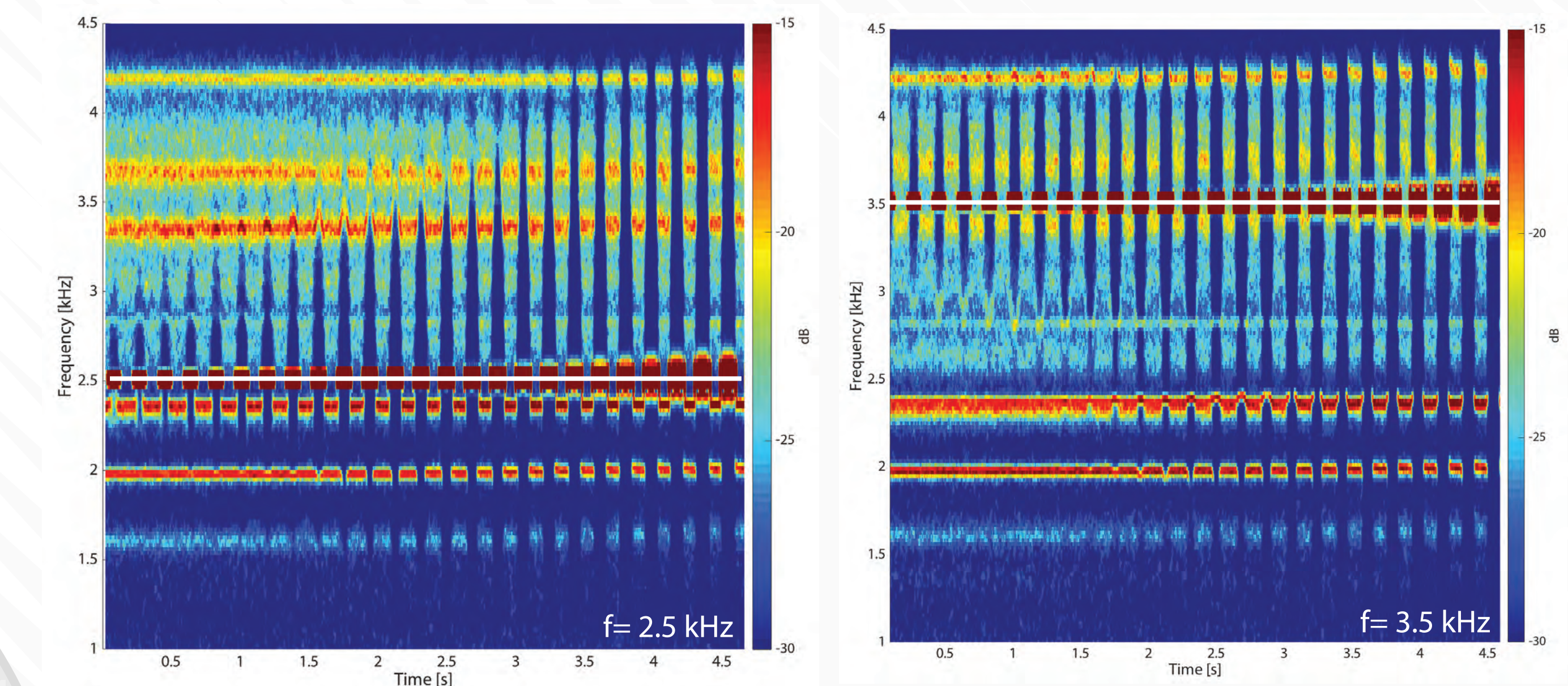


FIGURE 9 (Lizard) - Breaking the ring of fire w/ tone bursts of varying level. Spectrograms of tone burst swept across frequency at constant frequency (2.5 kHz on left, 3.5 kHz on right; indicated via horizontal white line). Bursts were 113 ms long, cosine-ramped. Spectrograms used a 2048 point window with 95% sliding overlap, spectrally averaged across 40 stimulus presentations. (same ear as shown in Fig.5,8)

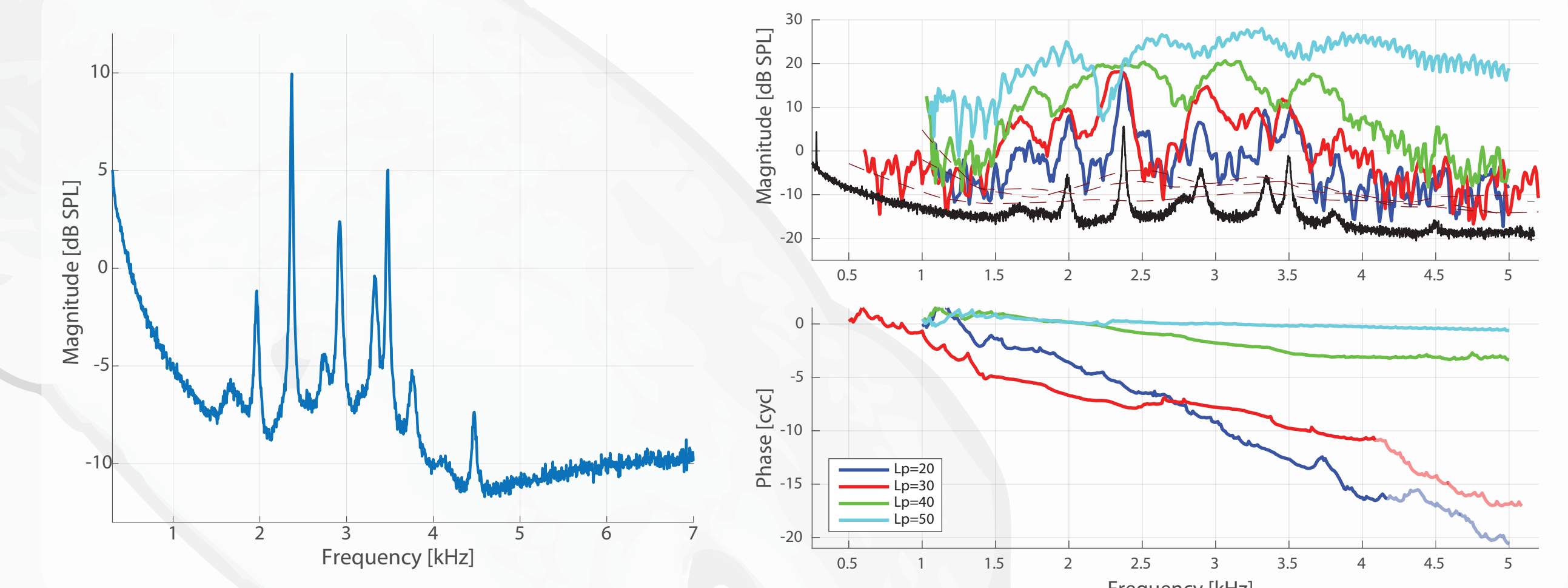
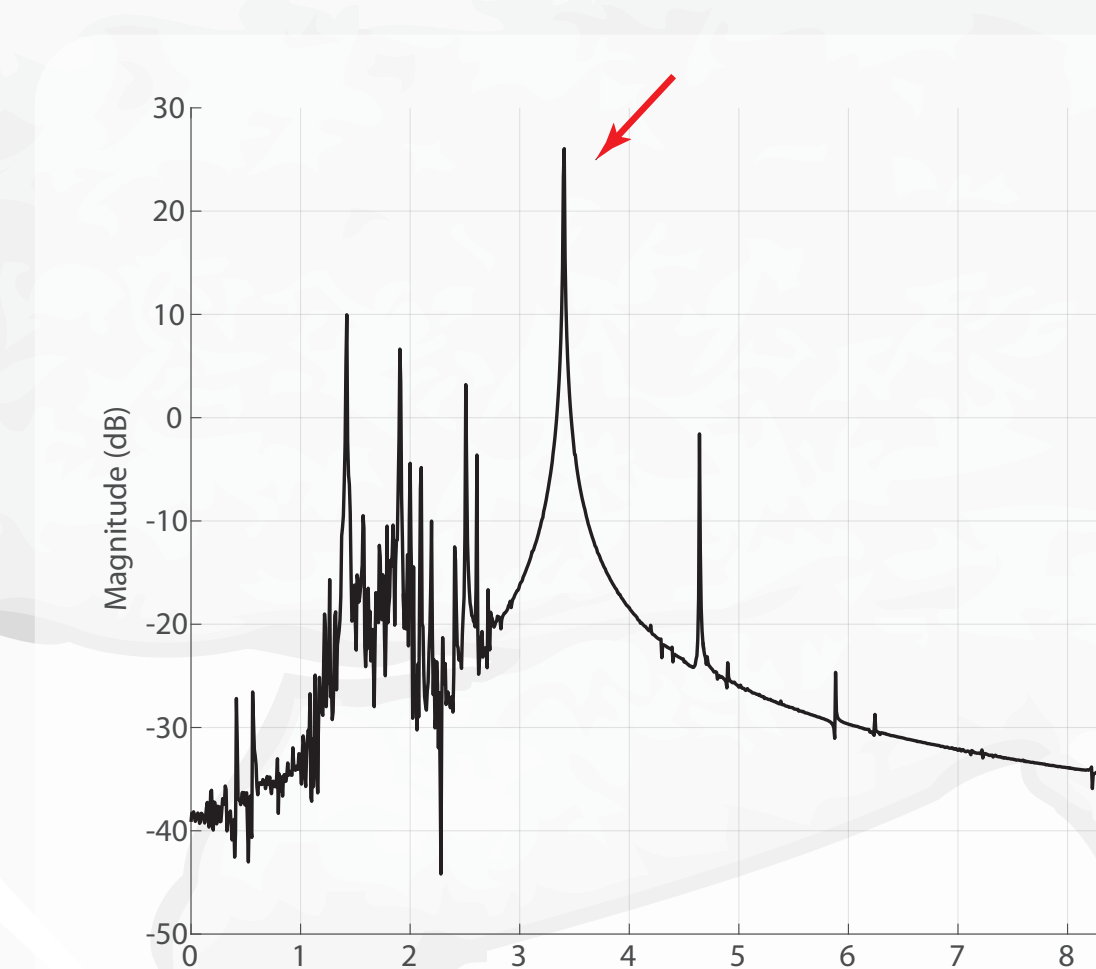


FIGURE 10 (Lizard) - Level-dependence of SFOAEs. A swept-tone and suppression paradigm was used ($f_s=f_p+40$ Hz, $L_s=L_p+15$ dB; Kalluri & Shera, 2013). SOAE spectrum for this lizard is shown on left and right (black curve). SFOAE noise floor indicated by brown dashed curves.

FIGURE 11 (Model) - Effect of an external tone (3.4 kHz, $L_i=L_j=0$). [Top] As indicated by the red arrow, a large response is apparent about the tone frequency. At lower frequencies, the clusters become broken up. [Bottom]. Spectra for all oscillators shows breaking up, as well as entrainment.

Future Directions

- Determine biomechanically-based bounds on relative parameter sizes (e.g., viscous versus reactive coupling, global vs nearest-neighbor coupling). Such can/should be tied back to "size" considerations (e.g., length of papilla)
- Appropriate inclusion of stochastic forces dynamically affecting bundles/papilla
- Allow for active control parameter (epsilon) to vary dynamically.
- Is this model "too simple"? Need to consider oscillators as 3rd order (or higher)?
- Determine what role (standing?) wave-behavior is playing

References

- Bergevin, C & Shera, CA (2010) JASA 127(4):2398-2409
- Bergevin, C et al. (2015) PNAS 112(11):3362-3367
- Duke, T & Julicher, F (2003) PRL 90: 158101
- Fruth, F et al (2014) Biophys. J. 107(4):815-824
- Gelfand, M et al. (2010) PLoS ONE e111116
- Hudspeth, AJ (2008) Neuron 59(4):530-545
- Johannesma, P (1980) Psych. Physiol. Behav. Stud. Hear. pgs.62-63
- Kalluri, R & Shera, CA (2013) JASA 134:3556
- Manley, GA (1996) JASA 99:1588-1603
- Salerno, A & Bergevin, C (2015) JASA 137: 2409
- Shera, CA (2003) J. Acoust. Soc. Am. 114(1):244-262
- Talmadge, CL et al. (1991) J. Acoust. Soc. Am. 89(5):2391-2399
- Vilfan, A & Duke, T (2008) Biophys. J. 95:4622-4630
- Wit, HP & van Dijk, P (2012) J. Acoust. Soc. Am. 132(2):918-926
- Wit, HP et al (2012) J. Acoust. Soc. Am. 132(5):3273
- Wit, HP (1985) Peripheral Auditory Mechanisms, pgs. 221-228

Acknowledgements

Support provided by the National Science and Engineering Research Council (NSERC)



YORK UNIVERSITY